LAWRENCE
LIVERMORE
NATIONAL
LABORATORY

LLNL-JRNL-581492

Optimized pitch button blocking for polishing high-aspect-ratio optics

M. D. Feit, R. P. DesJardin, W. A. Steele, T. I. Suratwala

September 14, 2012

Applied Optics

Disclaimer

Optimized pitch button blocking for polishing high-aspect-ratio optics

M.D. Feit*, R.P. DesJardin, W.A. Steele, T.I. Suratwala

Lawrence Livermore National Laboratory, P.O. Box 808, Livermore, CA 94551, USA

* Corresponding author: feit1@llnl.gov

Pitch button blocking (PBB), involving attaching small pitch buttons between the back of a thin workpiece (i.e. optic) and a blocking plate, enables non-compliant convergent polishing in which the workpiece stiffness and block interface strength are maintained. This process has been optimized and practical design criteria (number, size and spacing of pitch buttons) have been determined both experimentally and theoretically using a thermoelastic model.. The optimized PBB process has been successfully implemented on 100-265 mm sized workpieces with aspect ratios up to 45 resulting in a maximum peak-to-valley heights of <|0.1| μm after blocking and polishing.

OCIS codes: 220.5450, 220.4610, 160.2750

I. Introduction

Polishing pitch has been found useful in the manufacture of optics for hundreds of years, even being mentioned by Sir Isaac Newton in his 1704 “Opticks”. Pitch is a complex material exhibiting elastic, delayed elasticity, and creep properties. It has unique ability to hold a ‘charge’ by embedding polishing particles allowing for uniform load transfer to the workpiece, leading to material removal and smoothing at the nm level [1-3]. Also, the ability of pitch to creep or flow under load to match the surface being polished (flats or spheres) is the other key attribute for uniform removal over the part surface (when desired) and for figure control [1-3]. Preston discussed the important physical properties of pitch used for blocking lenses and the issue of thermal strain, in which he recommended not heating the pitch any more than absolutely necessary [4]. Brown investigated the temperature dependence of viscosity for common pitches and the difference between “soft” and “hard” pitches [1]. More recently, Degroote et al reported modern measurements of viscosity, softening point and hardness for a number of petroleum based and wood based pitches [5].

Pitch has been used not only as a medium to polish on (i.e., as a ‘lap’), but also as a blocking agent to hold workpieces (typically optics) for polishing. There are several methods for using pitch as a blocking medium [6-9]. One method uses a thin layer of pitch across the whole blocking plate to block single or multiple parallel workpieces. A second method blocks lens(es) to a curved blocking

tool with relatively thick full-aperture pitch button(s) on the back surface [6-9]. A third method, which is the focus of the following study, is referred to as pitch button blocking (PBB)[9] and involves attaching a number of small pitch buttons to an individual workpiece in order to block it without unduly distorting it, as often happens to high-aspect ratio workpieces (i.e., high width-to-thickness ratio).

Blocking such high-aspect workpieces using the first blocking method can result in scratching damage due to possible rogue particles or asperities at the workpiece/block interface [10,11]. Also, since pitch is applied over the entire back surface, the difference in thermal expansion between workpiece and pitch during cooling will lead to residual stresses that ultimately distort the workpiece. The amount of this distortion is analogous to the bending of a bimetallic strip. The classic analysis of Timoshenko [12] indicates that the peak-to-valley distortion in such a strip supported at the ends scales as the square of the length of the strip, i.e. as the square of the distance between support points. Thus to minimize distortion, it is attractive to break up the pitch layer into discrete buttons (as in PBB) separated by a distance small compared to the workpiece size.

During polishing it is often desirable to mount or block the workpiece such that it will not bend (i.e., remain stiff). This is especially the case for new polishing methods such as Convergent Polishing[13,14] where a workpiece, regardless of its initial surface, will converge the shape of the lap in a single iteration. An ideal PBB process would provide: 1) a minimum level of workpiece deformation during the blocking process, 2) enough interface strength to survive the shear forces during polishing to not delaminate, and 3) minimum creep or flow while under load during polishing to minimize workpiece bending during polishing. To date, PBB techniques have been largely practiced in an artisan manner. In other words, little is understood about the impact of the PBB process parameters on the degree of deflection of the workpiece and its corresponding survivability during polishing.

In the following study, two different workpiece materials (fused silica and phosphate glass) are PBB under a variety of process conditions (e.g., pitch material, process temperature, number of buttons, button size, and button spacing), and then the workpiece deflection during blocking and its effectiveness during polishing are measured. A simple thermoelastic model using an effective pitch thermal expansion coefficient to account for stress relaxations is used to quantitatively explain observed deflections as function of workpiece material and PBB geometry. Finally, a set of design criteria for PBB are proposed for various sized workpieces based on a minimum spacing between buttons and a minimal area fraction of buttons.

2. Experimental

Fused silica (Corning 7980 or Heraeus Suprasil 314) and phosphate glass (LHG-8, Hoya Corporation) workpieces (100 mm diameter x 2.2 mm thick) were initially finished by Bond Optics (Lebanon, NH) to less than 0.3 μm peak-to-valley surface figure. The workpieces were then PBB using the procedure schematically shown by Figure 1. First, tape (3M) was applied to surface S2 of the workpiece and to one surface of a stainless steel block (100 mm diameter x 25 mm thick). Then pitch droplets (formed by heating with a soldering iron) were applied to the taped surface of the block. The block with the pitch buttons was then placed into the oven and annealed. Next the

workpiece was placed on top of the buttons with taped surface S2 contacting the pitch, heated as needed, and covered to minimize convective flow heat transfer at the process temperature (T). Note the button volume was tailored by adjusting the number of pitch droplets applied for each button, and the button thickness was tailored by adjusting the oven heat time which systematically changed the button thickness (t_p) and diameter ($2r_p$) (for a fixed pitch volume). Finally, the workpiece-pitch button-block composite was slowly cooled to room temperature at a rate of ~10 ^oC/hr. The reflected wavefront of workpiece surface S1 was measured before blocking, after blocking, and sometimes after polishing using a 6" Zygo Veri Fire AT+ Fizeau interferometer. The workpiece deflection before and after blocking was quantified as the difference in the peak-to-valley height (ΔPV) where positive values signify more concave surfaces and negative values more convex surfaces. Note each measured peak-to-valley height is calculated as the maximum height difference on the measured surface after 1% of the low and high data points have been discounted to minimize sensitivity due to anomalous data points in the interferometry measurements.

PBB was performed using various pitch materials having differing softening temperatures including Gugolz 73 (G73), Gugolz 82 (G82), Cycad Brown Blocker Pitch (Cycad), and Universal Blocking Pitch #1 (BP1) (from Universal Photonics Inc., Hicksville, NY or Cycad Products, Las Vegas NM). The material properties of the pitches are shown in Table 1. Figure 2 is a schematic outlining PBB geometric parameters, including the number of buttons (N), the button spacing (d_m), the button radius (r_p), and the button thickness (t_p), which were varied for each PBB experiment. Table 2 lists the specific process parameters for each of the PBB experiments. Fused silica PBB experiments are labeled as S1-S26 and Phosphate glass PBB experiments as P1-P10. Also, experiments S1-S2 used Gugolz 73 pitch, S3-S14 used Gugolz 82 pitch, S15-S17 used the harder Cycad pitch, and S18-S26 and P1-P10 used BP1 pitch. Several larger fused silica workpieces (265 x 265 x 9 mm^3) were also PBB using BP1 with N=81, d_m=24 mm, r_p=3 mm, and t_p= 1.0 mm (not shown in Table 2). The reflected wavefront for the larger workpiece was measured using a larger Fizeau 12" interferometer (Zygo Mark GP1 XPS).

Some of the PBB workpieces were polished using cerium oxide slurry on a polyurethane pad using the Convergent Polishing method. The details of the polishing setup and procedure are described in detail elsewhere [13,14]. After polishing, the surface figure was measured before and after deblocking as described above.

The thermal expansion coefficients of some of the pitch materials were measured using thermal mechanical analysis (TMA) (Perkin Elmer). A pitch cylinder (5 mm diam x 3 mm thick) was mounted with a pin attached to the top. The linear expansion was measured by the pin position with increase in temperature.

3. Results

Figure 3a shows a photo of Sample S18, a 100 mm x 2.2 mm round fused silica workpiece PBB with 11 buttons showing low deflection. The same is shown in Figure 3b but for a larger square workpiece (265 x 265 x 9 mm^3) using similar design rules.

As discussed in the Experimental section, Table 2 summarizes the experiments carried out to investigate the influences of materials, number, dimensions, and types of pitch buttons on the workpiece deflection of high-aspect ratio fused silica and phosphate glass workpieces during blocking. The last column summarizes the deflection results, described as the change in Peak-to-Valley height in the reflected wavefront before and after blocking (ΔPV). Deflections varied dramatically depending on the PBB conditions from as low as 0.00 μm (i.e., not measurable) to ~10 μm. The largest deflections were observed using a single solid button covering the whole workpiece (Samples S14, S17, S25, S26, P9 & P10). Except for the single solid button cases, all the fused silica workpieces deflected convex (negative deflection), and conversely all the phosphate glass workpieces deflected concave (positive deflection). Figure 4 illustrates this, showing diameter lineouts of the change in surface figure for selected samples from Table 2. The defections were usually radially symmetric. In other words, a single lineout accurately describes the 2D measured surface, and the surface change can be described largely as Power.

The change in surface figure (ΔPV) of all of the fused silica PBB configurations listed in Table 2 is plotted in Figure 5a as a function of the spacing between the pitch buttons (d_m). The magnitude of ΔPV decreases continuously with increasing d_m which was largely insensitive to the other pitch button parameters In fact, there are two regimes: for d_m<10 mm, the rate of decrease of deflection with d_m is large; and for d_m>15 mm, the rate of decrease of deflection with d_m is small. Figure 5b shows the change in surface figure (ΔPV) of all of the fused silica and phosphate PBB workpieces as a function of the of the area fraction of buttons (A_f) when d_m>15mm. Here the deflections (all relatively small) nominally increase linearly with area fraction of buttons (A_f).

Figure 6 shows the results for the linear expansion of two of the pitches used in this study (Cycad and BP1). Both pitches had similar and relatively high thermal expansion coefficients (~$40x10^{-6}$ $^oC^{-1}$) which are summarized in Table 1.

4. Discussion

4.1 Thermoelastic Model

When elastic materials of differing mechanical and thermal properties are joined together at a working temperature initially without stresses and then cooled to room temperature, the net response of the system can be described by thermo-elastic equations accounting for overall balance of forces [15]. In particular, the constitutive equations may be formulated in terms of the displacement vector (u,v,w) which describes the displacement from the initial state in the (x,y,z) directions as a function of position and utilizes the equivalence of a constant temperature state with distributed body forces and an equivalent thermo-elastic state with forces provided by thermal stresses [15]. These elastic displacements are given in each material by solving [15]:

$$\frac{(1+2\nu)}{(1+\nu)(1-2\nu)}E\frac{\partial e}{\partial x}+\frac{E}{2(1+\nu)}\nabla^2 u-\frac{E}{(1-2\nu)}\alpha\frac{\partial T}{\partial x}=0$$
$$\frac{(1+2\nu)}{(1+\nu)(1-2\nu)}E\frac{\partial e}{\partial y}+\frac{E}{2(1+\nu)}\nabla^2 v-\frac{E}{(1-2\nu)}\alpha\frac{\partial T}{\partial y}=0 \quad (1)$$
$$\frac{(1+2\nu)}{(1+\nu)(1-2\nu)}E\frac{\partial e}{\partial z}+\frac{E}{2(1+\nu)}\nabla^2 w-\frac{E}{(1-2\nu)}\alpha\frac{\partial T}{\partial z}=0$$

along with solving for the temperature T from the steady state heat equation:

$$k\nabla^2 T=0. \quad (2)$$

Each material is described in terms of elastic modulus (E), Poisson ratio (ν), thermal expansion coefficient (α), and thermal conductivity (κ). The local volume dilation (e) is given by:

$$e=\frac{\partial u}{\partial x}+\frac{\partial v}{\partial y}+\frac{\partial w}{\partial z} \quad (3)$$

The thermoelastic equations (Eqs. 1-3) were solved using the FlexPDE (PDE Solutions Inc, Spokane Valley, WA 99206) partial differential equation solver for a typical workpiece with pitch buttons geometry as shown schematically in Fig. 2 with specific PBB parameters outlined in Table 2. The material properties used in the simulations are summarized in Table 3. The boundary between the pitch and the block was simulated as fixed boundary. The initially stress-free composite system was cooled from the processing temperature to room temperature. In practice, a small temperature gradient in the z direction is useful for numerical convenience in determining the steady state solution in calculating gradients and Laplacians, and there is no heat flow through the sides of the materials. The output from the simulation consisted of the final displacements (u,v,w) from which the ΔPV of the non-pitch buttoned side of the workpiece was determined before and after blocking allowing for direct comparison with the experimental results in Table 2.

4.2. Model Comparison with Experiment and Sensitivity Study

Since the thermal stresses depend on the differential thermal expansion between the workpiece and pitch, the resulting workpiece deflection is expected to be proportional to the difference in thermal expansion coefficients. Fused silica has a very low thermal expansion coefficient of $0.54\text{x}10^{-6}\ ^{o}C^{-1}$, while phosphate glass has a larger thermal expansion coefficient of $12.7\text{x}10^{-6}\ ^{o}C^{-1}$ (see Table 3). If the thermal expansion of pitch is larger than that of the phosphate glass, both glasses should have the same sign of ΔPV with the silica being larger in magnitude. On the other hand, if the pitch thermal expansion coefficient lies between that of fused silica and phosphate glass, the ΔPV should have opposite signs for the two glasses.

As discussed in the Results Section, the thermal expansion coefficients of the two pitches in this study were $\sim 40\text{x}10^{-6}\ ^{o}C^{-1}$, larger than both the phosphate glass and fused silica glass. This would indicate both glasses should exhibit the same sign of ΔPV, which is in contradiction to the experimental observations with multiple buttons (see Fig. 5). Also, using this value of the pitch thermal expansion coefficient also led to calculated values of the deflection using the thermoelastic model that are much larger in magnitude than the experimental data. The above model assumed perfectly elastic behavior while pitch is known to stress relax. Rather than developing a more

complex stress-relaxation model, we decided to account for relaxation effects by using an effective pitch thermal expansion coefficient. Using a pitch thermal expansion coefficient of 2.4×10^{-6} C^{-1} led to a consistent prediction of the ΔPV's for both fused silica and phosphate glass workpieces as shown in Fig. 5b.

Using the thermoelastic model with the revised effective pitch thermal expansion coefficient, a systematic sensitivity study was then conducted to gain insight on the effect of various process variables on the PBB deflection. The model results are summarized in Figures 7a-d for PBB a fused silica workpiece (100 mm diam x 2.2 mm thick). Figure 7a illustrates that decreasing the degree of undercooling of the pitch leads to less deflection. Hence it is best to use the minimum process temperature tolerable. A pitch with a lower softening temperature (e.g. G72) would provide this. However, this could be at the expense of creep during polishing (see Section 4.3). Figure 7b shows the change in surface figure upon blocking a single button as a function of button size. As the button size gets smaller, the deflection decreases dramatically. Also, shown in Figure 7b is the sensitivity of the deflection to changes in pitch properties. As expected, deflection decreases with decreasing pitch modulus, pitch thermal expansion coefficient, and pitch thickness. Figure 7c shows the simulation results for change in surface figure as a function of area fraction of pitch (A_f) (using 3 and 9 buttons of various pitch button sizes while keeping d_m>15 mm). These results show a linear dependence of the deflection with area fraction, matching the behavior observed experimentally (shown in Fig. 5b). Finally in Figure 7d, the calculated ratio of the change in surface figure to the area fraction ($\Delta PV/A_f$) is plotted against the button spacing (d_m). The calculations show that this ratio is essentially constant for d_m>15 mm, but increases when d_m<15 mm, again consistent with the results shown in Fig. 5a.

With some confidence that the thermoelastic model captures the salient characteristics expected and observed experimentally, the model was now applied to simulate the specific experiments conducted in this study (Table 2). Figure 5b shows the results of the simulation (using the $\alpha_p = 2.4 \times 10^{-6}$ $^oC^{-1}$) as represented by the lines for fused silica and phosphate glass workpieces. Again, the thermoelastic model simulation shows: 1) the deflection scales linearly with area fraction (A_f) of pitch button; 2) the correct sign of the deflection with changes in workpiece thermal expansion coefficient; and 3) reasonable quantitative agreement of the magnitude of deflection (ΔPV) observed.

The change in surface figure (ΔPV) for small relative area fraction (A_f) cannot be simply extrapolated to large relative area (i.e. A_f approaching 1). The single button results reported in Table 2 and Figure 4 all indicate an overall increased concavity for both fused silica and phosphate glasses regardless of pitch used. Additionally, the magnitude of change for fused silica is larger than one might expect from the small relative area results. The fact that the single button behavior is relatively independent of the glass thermal expansion suggests that the pitch properties are predominant in determining the behavior. Since the same cooling schedule was used in all cases, larger buttons will have a greater non-uniform temperature distribution during cooling with the core warmer than the outer skin. It seems likely that the thermal gradient will be "frozen in" in terms of a resultant stress pattern that leads to concavity regardless of the workpiece material for PBB using a large area fraction of buttons (A_f).

4.3 Polishing Performance using PBB

The optimum pitch button blocking (PBB) design for high aspect ratio workpieces would fulfill the follow criteria: 1) minimize the deflection (ΔPV) as a result of blocking the workpiece; 2) provide sufficient interface strength such that during polishing the block does not delaminate; and 3) maximize the stiffness of the block such that workpiece does not bend under load while polishing. In order to maximize the stiffness of the block and interface strength, one can use a single button covering the all of the interface between the workpiece and the block; however, this would be done at the expense of getting a large deflection of the workpiece (as demonstrated by Samples S14,S17, S25, S26, P9, and P10 (see Table 2)). At the other extreme, applying a small, single button in the center would minimize deflection (ΔPV) during blocking at the expense stiffness and interface strength. The optimum is somewhere in between.

In a recent study [13,14], the concept of Convergent Polishing was introduced and demonstrated, where a workpiece regardless of its initial surface figure will converge to the lap shape in a single iteration. This technique requires that all the sources of material removal non-uniformity be removed, except for the workpiece-lap mismatch due to the workpiece surface shape. For a high aspect ratio workpiece, its bending upon loading on the polisher can prevent such a technique from working. Hence, low deflection PBB is an attractive blocking method for Convergent Polishing.

To test if a low area fraction of pitch at the interface (A_f) has enough strength to withstand the polishing run, the Convergent Polishing technique was conducted using Sample S21 (fused silica workpiece, N=11 buttons, r=6.5, A_f=0.05). This blocked workpiece survived polishing over 10's of hours with A_f =0.05, confirming it had sufficient interface strength. Figure 8 compares the workpiece surface figures before and after polishing using the optimized PBB process (Sample S21) with using a foam blocking process before and after polishing [13]. Note that the PBB workpiece surface figure converged to flat while the foam blocked workpiece did not change surface figure before and after polishing. This indicates that the foam blocked workpiece bends during polishing resulting in uniform spatial material removal while the PBB workpiece was stiff leading to non-uniform material removal due to workpiece-lap mismatch [13].

To test for pitch creep induced workpiece deflecture during polishing loading, Samples S21 and P1 were polished for 10+ hrs and then the deflection was determined as the reflected wavefront after polishing (blocked) minus the reflected wavefront after polishing (unblocked). These results showed minimal workpiece peak-to-valley deformation and hence creep after polishing (<|0.03| μm for fused silica (Sample S21) and <|0.08| μm for phosphate glass (Sample P1)).

4.4 Design Rules for Optimum PBB

As discussed earlier, both the experimental results and the thermoelastic model calculations show that as A_f is decreased, the amount of workpiece deflection during blocking is decreased (see Figures 5b & 7d). Also, for the thicknesses of the workpieces explored in this study, a button offset (d_m) >15 mm is sufficient to minimize the 'crosstalk' between buttons contributing workpiece blocking deflection at a fixed A_f (see Figure 7c). With these guidelines, the following engineering design rules are proposed to optimize the PBB geometry (namely button size (r_p) and number of buttons (N)) to maximize the benefit of each of the criteria discussed in Section 4.3:

$$r_p = \frac{d_m}{\sqrt{\frac{\pi}{A_f}} - 2} \tag{4}$$

$$N = \frac{\pi r_w^2}{(2r_p + d_m)^2} \tag{5}$$

$$\Delta PV = A_f C \tag{6}$$

where r_w is the radius of the circular workpiece, and C is the linear rate of increase in deflection with area fraction (A_f) for a given system. From Figure 5b, C= +4.3 μm for phosphate glass and C= -0.56 μm for fused silica glass.

To illustrate the use of the design rules, consider A_f=0.05 as sufficient to have enough interfacial strength to survive polishing as determined in Section 4.3. Hence from Eq. 6, the ΔPV upon blocking expected would be -0.03 μm for fused silica and 0.22 μm for phosphate glass as long as d_m>15 mm. For some added margin on minimizing crosstalk, we chose d_m=20 mm. Note keeping d_m small aids in increasing the stiffness of the workpiece. Using d_m=20 mm and A_f=0.05, Eqs. 4 and 5 can be solved for the ideal button radius (r_p) and number of buttons (N). This gives a button size of r_p=3.3 mm and N as shown in Figure 9 for various size workpieces. For a 50 mm radius workpiece (i.e., those used in this study), N=11. Application of PBB to larger workpieces will necessarily involve many more buttons. Hence practical routine application of PBB would benefit from a quick and reliable technique [16] to dispense uniform sized buttons on a pre-determined grid.

5. Summary

Pitch button blocking (PBB) is an age-old artisan method of blocking (i.e., holding) a workpiece for single-sided optical polishing. In cases where the workpiece can bend (i.e., a high aspect ratio workpiece) during polishing, it is often desirable to block the workpiece to make it stiff. An ideal blocking process: 1) would provide a minimum level of workpiece deformation during the blocking process; 2) would have enough strength to survive the shear forces during polishing; and 3) would have maximum stiffness to prevent deformation during polishing. In the present study, the workpiece deformation of high aspect-ratio fused silica and phosphate workpieces (100 mm in diameter x 2.2 mm thick) were measured interferometrically after PBB using a systematic set of processing conditions (e.g., pitch material, temperature, and pitch button geometry (number, size, and spacing)). The results show that the amount of workpiece deformation increased linearly with areal fraction of pitch (A_f) when the button offset spacings (d_m) were >15 mm. With d_m<15 mm, however, workpiece deformation increased non-linearly towards the amount of deformation observed in a single solid button (A_f=1). A thermoelastic model of the PBB process (which uses an effective pitch thermal expansion coefficient to account for stress relaxation effects) quantitatively describes the direction and magnitude of the deformation observed experimentally for both glass types as a function of A_f and d_m. Performing PBB using a higher temperature pitch and an A_f=0.05

provided minimal blocking deflections (<|0.10| μm). In addition, this configuration survived polishing and led to minimal workpiece peak-to-valley deformation after polishing (<0.03 μm for fused silica and <0.08 μm for phosphate glass). Finally, a set of useful design rules were described to apply optimized PBB geometry to various size workpieces.

6. Acknowledgements

The authors would like to thank Dr. Stephen Letts for performing the TMA analysis to determine the thermal expansion measurements of the pitch materials. This work was performed under the auspices of the U.S. Department of Energy by Lawrence Livermore National Laboratory with the Laboratory Directed Research & Development (LDRD) program under contract DE-AC52-07NA27344. LLNL-JRNL-581492.

References

1. N. Brown, "Optical polishing pitch", Optical Society of America workshop on Optical Fabrication and Testing, November 10-12, 1977, LLNL report UCRL-80301 (1977).

2. B. Gillman, F. Tinker, "Fun facts about pitch and the pitfalls of ignorance", *Proc. SPIE* **3782**, 72-79 (1999).

3. R. Varshneya, J.E. DeGroote, L.L. Gregg and S.D. Jacobs, "Characterizing optical polishing pitch", *Optifab 2003* (SPIE, Bellingham, WA) **TD02**, 87-89 (2003).

4. F.W. Preston, "On the properties of pitch used in working optical glass", *Trans. Opt. Soc.* **24** (3), 9117-9142, (1923).

5. J. E. DeGroote, S. D. Jacobs, L. L. Gregg, A. E. Marino, and J. C. Hayes, "Quantitative Characterization of Optical Polishing Pitch," *Proc. SPIE* **4451**, 209-22 (2001).

6. F. Twyman, *Prism and Lens Making* 2nd ed., (Adam Hilger, Bristol and New York, 1988).

7. D.F. Horne, *Optical Production Technology*, (Crane, Russak, & Co, New York, 1972).

8. H. Karow, *Fabrication Methods for Precision Optics*, (John Wiley & Sons, New York, 1993).

9. R. Scott, "Optical Manufacturing," *Applied Optics and Optical Engineering*, Vol. III, ed., R. Kingslake, (Academic Press, New York, 43–95, 1965).

10. T. Suratwala, M. Feit, J. Menapace, "Scratch Forensics", *Optics and Photonics News* **19**, 12-15 (Sept 2008).

11. T. Suratwala, R. Steele, M. Feit, L. Wong, P. Miller, J. Menapace, P. Davis, "Effect of Rogue particles on the sub-surface damage of fused silica during grinding/polishing", *J. of Non-Crystal. Solids* **354**, 2023-2037 (2008).

12. S. Timoshenko, "Analysis of bi-metal thermostats", *J. Opt. Soc. Am.* **11**, 233 (1925).

13. T. Suratwala, R. Steele, M. Feit, R. Desjardin, D. Mason, "Convergent Pad Polishing of Amorphous Silica", *International Journal of Applied Glass Science* **3**, 1-15 (2012).

14. T. Suratwala, W. Steele, M. Feit, R. Desjardin, D. Mason, R. Dylla-Spears, L. Wong, P. Miller, P. Geraghty, "Method and System for Convergent Polishing" *US Provisional Patent Application 61454893* (March 21,2011).

15. B.A. Boley and J.H. Weiner, *Theory of thermal stresses*, (John Wiley & Sons, New York,1960)

16. R. DesJardin, "Automated Pitch Button Dispensing Station and Method" US Patent 6692573 (Feb 17 2004).

Table 1: Properties of the pitch materials used in this study [2,3].

Pitch Material	Name	Melting Temperature (C)	Softening Temperature (C)	Shore Hardness D	Elastic Modulus E_p (GPa)	Thermal Expansion Coefficient $\alpha(oC^{-1})$
G73	Gugolz 73	78	72	79	0.24	--
G82	Gugolz 82	80	76	77	0.23	--
Cycad	CyCad Brown Blocking Pitch	73	66	--	--	$37x10^{-6}$
BP1	Universal Blocking Pitch #1	73	67	--	--	$43x10^{-6}$

Table 2: Summary of PBB experiments showing process parameters measured change in surface figure (ΔPV) before and after blocking. Note all workpieces were 100 mm in diameter and 2.2 mm thick.

Exp	Workpiece	Pitch	Process Temp (C)	# of Buttons N	Button Thick, t_p(mm)	Button Diameter, $2r_p$ (mm)	Button spacing, d_m (mm)	Area Fraction	ΔPV (μm)*
S1	FS	G73	65	37	1	10	4.6	0.370	-0.15
S2	FS	G73	65	37	1	10	4.6	0.370	-0.44
S3	FS	G82	72	3	1	10	41.2	0.030	-0.01
S4	FS	G82	72	4	1	9	35.3	0.032	0.00
S5	FS	G82	72	9	1.2	8	21.5	0.058	-0.06
S6	FS	G82	72	21	1.1	9	10.3	0.170	-0.08
S7	FS	G82	72	21	1.2	8	11.3	0.134	0.00
S8	FS	G82	72	37	1.1	11	3.6	0.448	-1.00
S9	FS	G82	72	37	0.9	12	2.6	0.533	-0.60
S10	FS	G82	72	37	0.8	13	1.6	0.625	-1.52
S11	FS	G82	72	37	1	11	3.6	0.448	-0.60
S12	FS	G82	72	37	0.7	14	0.6	0.725	-1.20
S13	FS	G82	72	37	0.8	11	3.6	0.448	-1.20
S14	FS	G82	78	1	2	NA	NA	1.000	1.73
S15	FS	Cycad	75	37	1.2	8	6.6	0.237	-0.33
S16	FS	Cycad	75	37	1.3	7	7.6	0.181	-0.26
S17	FS	Cycad	92	1	1.3	NA	NA	1.000	5.53
S18	FS	BP1	60	11	0.85	5	21.7	0.028	0.00
S19	FS	BP1	60	11	0.7	4.5	22.2	0.022	-0.10
S20	FS	BP1	60	11	0.7	4.5	22.2	0.022	-0.02
S21	FS	BP1	60	11	1.35	6.5	20.2	0.046	-0.04
S22	FS	BP1	60	11	1.4	9	17.7	0.089	-0.03
S23	FS	BP1	60	11	1.5	11.5	15.2	0.145	-0.18
S24	FS	BP1	60	37	0.75	9	5.6	0.300	-0.15
S25	FS	BP1	105	1	0.5	NA	NA	1.000	4.90
S26	FS	BP1	105	1	0.8	NA	NA	1.000	6.40
P1	P	BP1	60	11	0.6	4.5	22.2	0.022	0.04
P2	P	BP1	60	11	0.9	4.5	22.2	0.022	0.03
P3	P	BP1	60	11	0.8	6.5	20.2	0.046	0.23
P4	P	BP1	60	21	0.6	5	14.3	0.053	0.43
P5	P	BP1	60	11	1	7.5	19.2	0.062	0.28
P6	P	BP1	63	11	0.6	9	17.7	0.089	0.46
P7	P	BP1	70	11	0.4	13.5	13.2	0.200	1.10
P8	P	BP1	60	37	0.55	8	6.6	0.237	1.10
P9	P	BP1	105	1	0.5	NA	NA	1.000	7.90
P10	P	BP1	105	1	0.85	NA	NA	1.000	9.90

P= Phosphate Glass; FS= fused silica; NA= not applicable; *sign convention (negative is convex, positive is concave)

Table 3: Summary of material properties used in thermoelastic model for PBB.

Property	Variable (units)	Fused Silica	Phosphate Glass	Pitch
Elastic Modulus	**E (GPa)**	**73**	**50**	**0.22**
Poisson's ratio	**V**	**0.17**	**0.26**	**0.20**
Thermal Conductivity	**K (W/m K)**	**1.38**	**0.58**	**100***
Thermal Expansion Coefficient	**α ($x10^{-6}$ $^{o}C^{-1}$)**	**0.54**	**12.7**	**2.4****

*Estimate value; **effective thermal expansion coefficient used to compensate for stress relaxation effect (measured value ~$40x10^{-6}$ $^{o}C^{-1}$)

Figure Captions

Figure 1. Schematic illustrating the process steps for pitch button blocking (PBB).

Figure 2. Schematic of PBB parameters (material and geometric). Workpiece (w) and pitch (p) are each characterized by elastic modulus E, thermal expansion coefficient α, thickness t. and radius r. The spacing between pitch button centers is s while the separation between button edges is d_m.

Figure 3. Photographs of optimized PBB pattern used (a) for 100 mm diameter round fused silica workpiece (Sample S21)) and (b) for a 265 mm square fused silica workpiece.

Figure 4. Lineouts of the measured change in surface figure of fused silica and phosphate glass (100 mm diameter x 2.2 mm thick) in various blocking configurations (optimized PBB, un-optimized PBB, and solid blocking).

Figure 5. (a) Measured change in surface figure (ΔPV) of fused silica (100 mm diameter x 2.2 mm thick) in various PPB configurations as a function of button spacing (d_m); (b) Measured change in surface figure (ΔPV) of fused silica and phosphate glass workpieces (100 mm diameter x 2.2 mm thick) as a function of area fraction (A_f) when d_m<15 mm. The points represent experimental data and the line is the model fit using $\alpha_p = 2.4 \times 10^{-6}\ K^{-1}$.

Figure 6. Measured linear thermal expansion of BP1 and Cycad Pitch by thermal mechanical analysis.

Figure 7. Calculated change in surface figure (ΔPV) for various PBB scenarios on fused silica workpieces (d_w=100 mm diameter, t_w=2.2 mm, E=73 GPa, $\alpha = 5.4 \times 10^{-7}\ ^oC^{-1}$). (a) Calculated ΔPV after PBB as a function of degree of undercooling of the pitch for single button (r=50 mm) and 3 button (s=50 mm; r_p=5 mm); (b) Calculated ΔPV after PBB for single button case and various pitch moduli, thickness, and thermal expansion coefficients (ΔT=54 ^oC); (c) Calculated ΔPV for various 3 & 9 button PBB as a function of A_f (where d_m>15 mm); (d) Calculated ΔPV/A_f after PBB as a function of button separation distance (d_m) for 3 and 9 button simulations at various button sizes (ΔT=54 ^oC, t=1 mm; E_p=0.22 GPa; $\alpha_p = 5.4 \times 10^{-6}\ ^oC^{-1}$); The lines in (c) and (d) represent simple empirical curve fits of the simulation results.

Figure 8. Surface figure of fused silica workpiece (100 mm x 2.2 mm thick) using pitch (stiff) button blocking (Sample S21) (a) before and (b) after polishing (full scale -18 to 5 μm); Surface figure of fused silica workpiece (100 mm x 2.2 mm thick) using foam (compliant) blocking (c) before and (d) after polishing (full scale-8.0 μm to 6.0 μm) (after ref [**Error! Bookmark not defined.**] with permission).

Figure 9. Calculated number of buttons for optimized PBB using spacing d_m=20 mm and relative area A_r=0.05 as a function of workpiece radius using Eqs. 4-5.

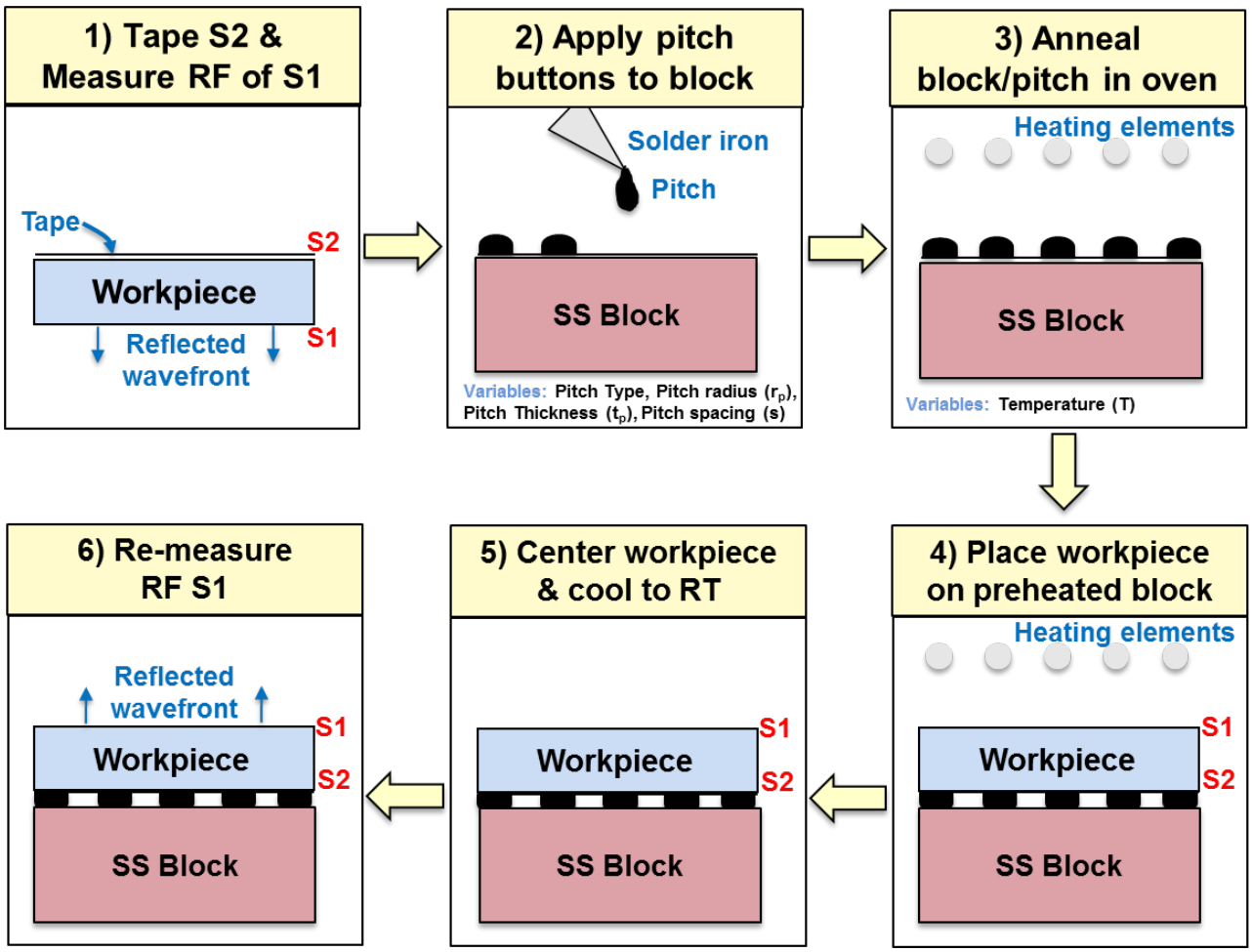
1) Tape S2 & Measure RF of S1
Tape
S2
Workpiece
S1
Reflected wavefront
2) Apply pitch buttons to block
Solder iron
Pitch
SS Block
Variables: Pitch Type, Pitch radius (r_p), Pitch Thickness (t_p), Pitch spacing (s)
3) Anneal block/pitch in oven
Heating elements
SS Block
Variables: Temperature (T)
4) Place workpiece on preheated block
Heating elements
S1
Workpiece
S2
SS Block
5) Center workpiece & cool to RT
S1
Workpiece
S2
SS Block
6) Re-measure RF S1
Reflected wavefront
S1
Workpiece
S2
SS Block

Figure 1.

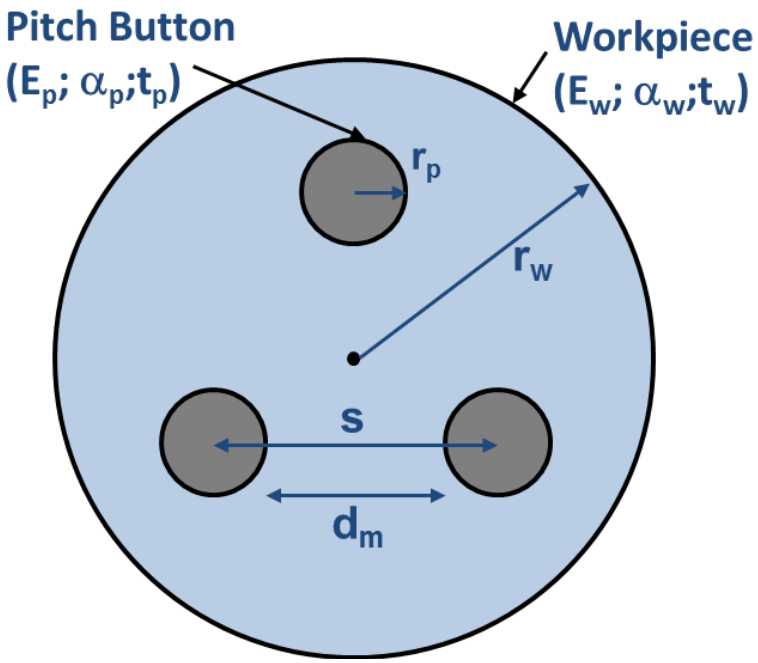

Figure 2.

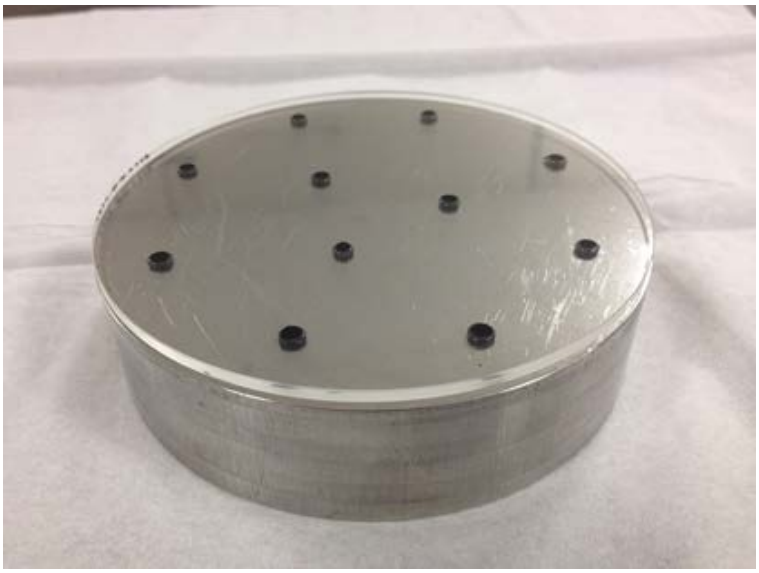

(a)

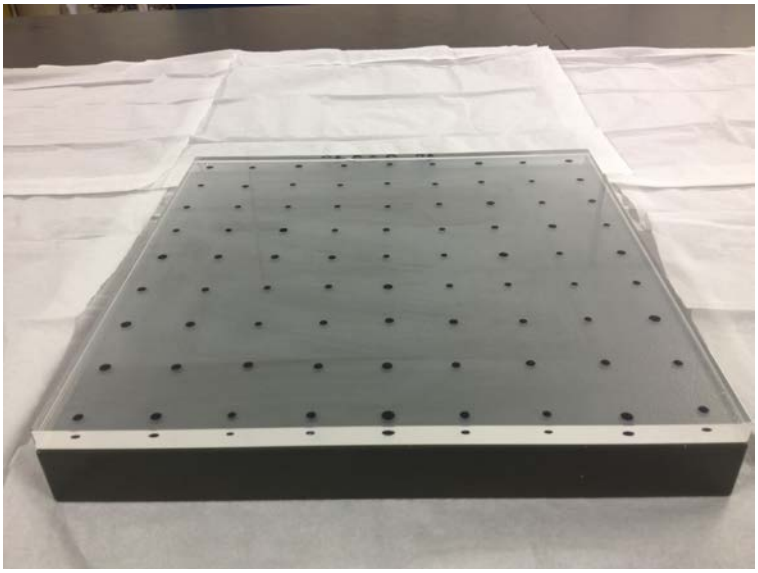

(b)

Figure 3.

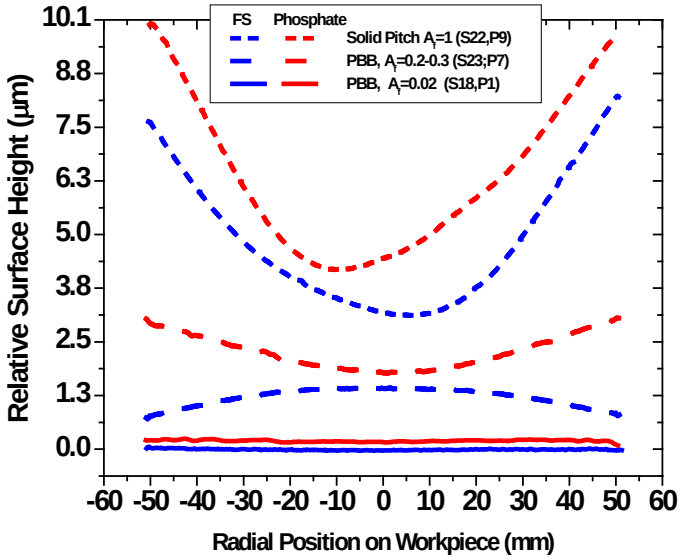
FS Phosphate
Solid Pitch A_T=1 (S22,P9)
PBB, A_T=0.2-0.3 (S23;P7)
PBB, A_T=0.02 (S18,P1)
Relative Surface Height (µm)
10.1
8.8
7.5
6.3
5.0
3.8
2.5
1.3
0.0
-60 -50 -40 -30 -20 -10 0 10 20 30 40 50 60
Radial Position on Workpiece (mm)

Figure 4.

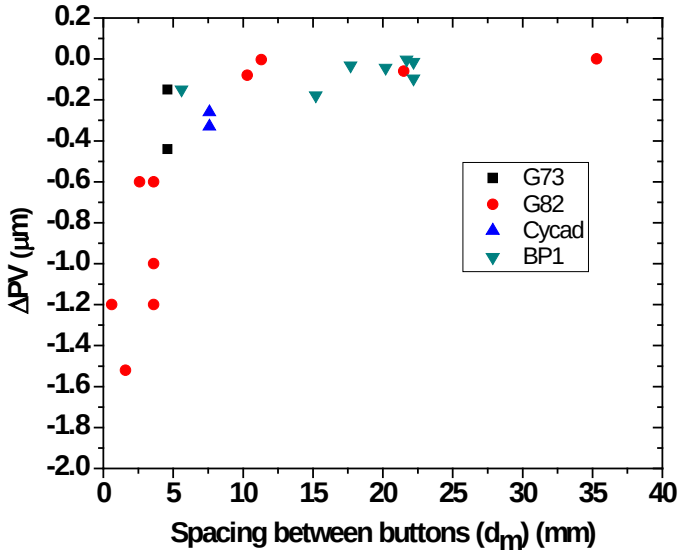
ΔPV (μm)
Spacing between buttons (d_m) (mm)
G73
G82
Cycad
BP1

(a)

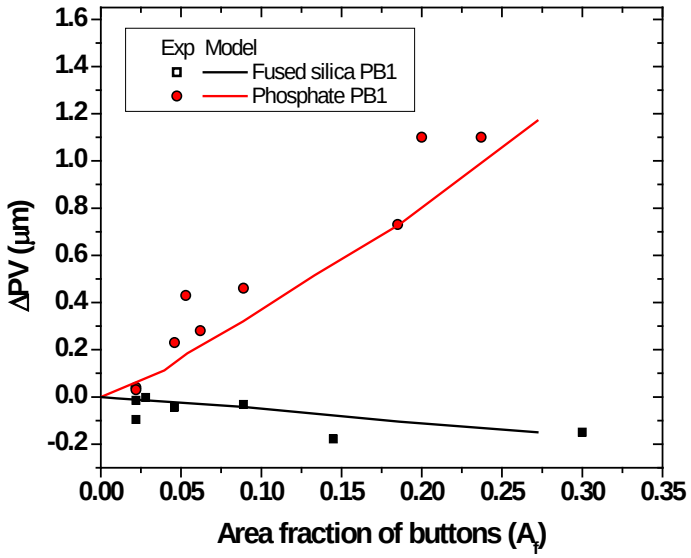
ΔPV (μm)
Area fraction of buttons (A_f)
Exp Model
Fused silica PB1
Phosphate PB1

(b)

Figure 5.

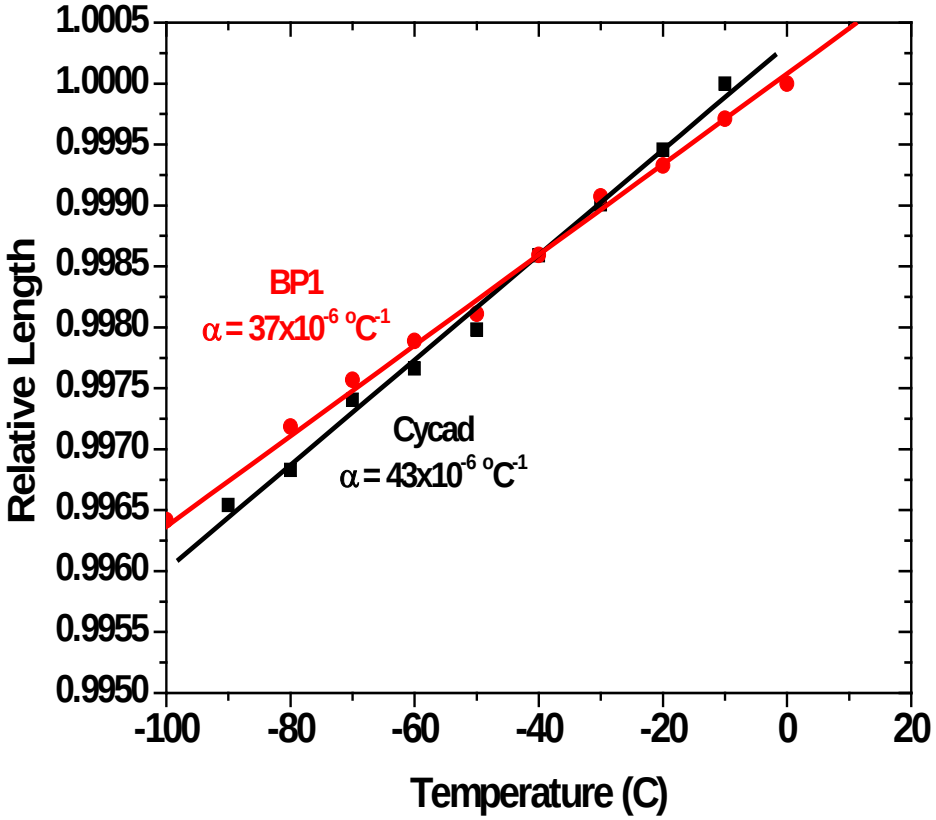
1.0005
1.0000
0.9995
0.9990
0.9985
0.9980
0.9975
0.9970
0.9965
0.9960
0.9955
0.9950
Relative Length
BP1
α = 37x10-6 °C-1
Cycad
α = 43x10-6 °C-1
-100
-80
-60
-40
-20
0
20
Temperature (C)

Figure 6.

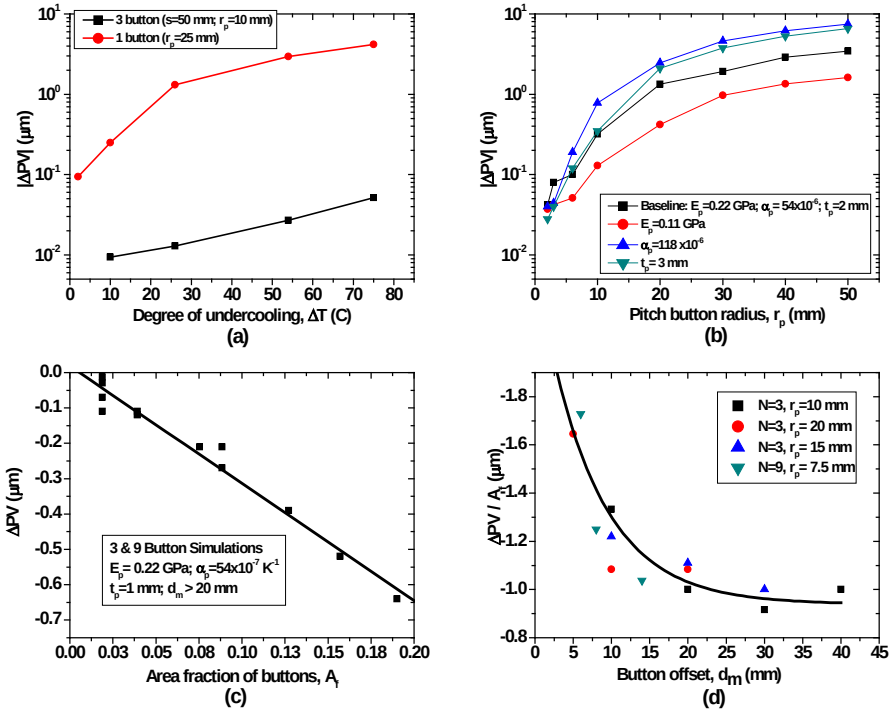
3 button (s=50 mm; r_p=10 mm)
1 button (r_p=25 mm)
|ΔPV| (μm)
Degree of undercooling, ΔT (C)
(a)
Baseline: E_p=0.22 GPa; α_p=54x10^-6; t_p=2 mm
E_p=0.11 GPa
α_p=118 x10^-6
t_p= 3 mm
Pitch button radius, r_p (mm)
(b)
ΔPV (μm)
3 & 9 Button Simulations
E_p= 0.22 GPa; α_p=54x10^-7 K^-1
t_p=1 mm; d_m > 20 mm
Area fraction of buttons, A_f
(c)
N=3, r_p=10 mm
N=3, r_p= 20 mm
N=3, r_p= 15 mm
N=9, r_p= 7.5 mm
ΔPV / A_f (μm)
Button offset, d_m (mm)
(d)

Figure 7.

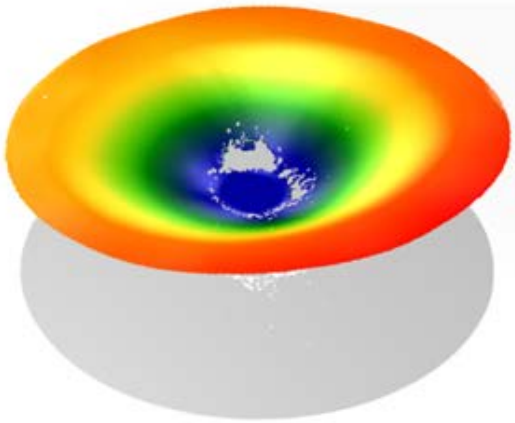

PBB workpiece (Sample 21) before polishing
PV= 22.5 μm
(a)

PBB workpiece (Sample 21) after polishing
PV= 0.31 μm
(b)

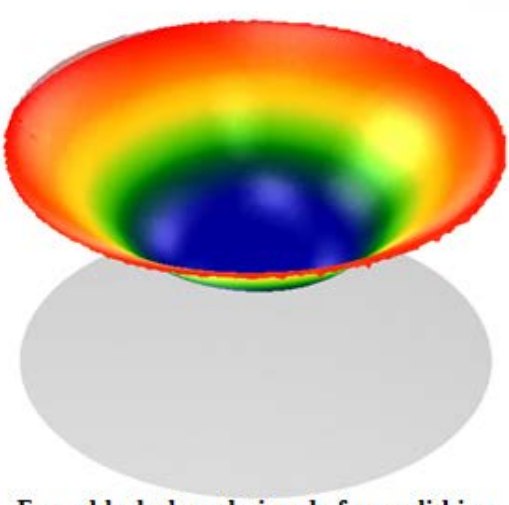

Foam blocked workpiece before polishing
PV_q= 13.8 μm
(c)

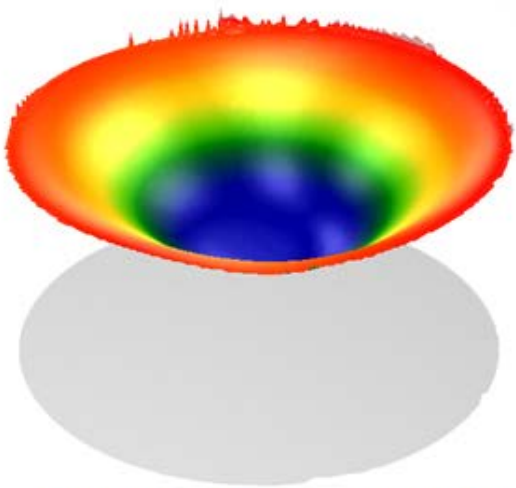

Foam blocked workpiece after polishing
PV_q= 12.3 μm
(d)

Figure 8.

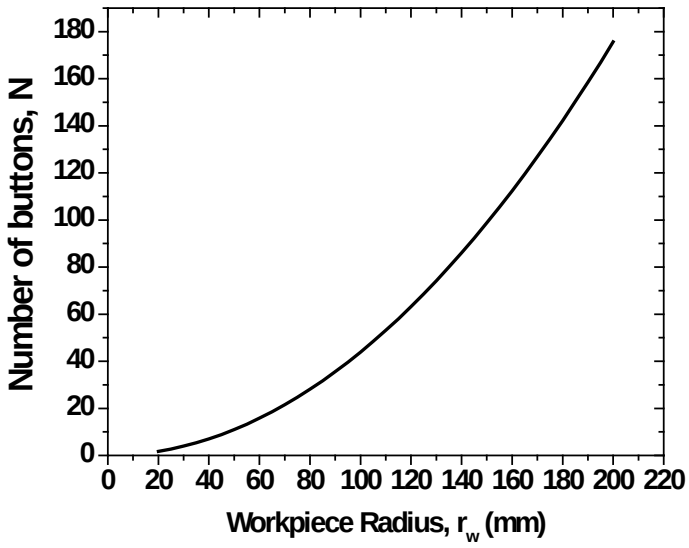
Number of buttons, N
0
20
40
60
80
100
120
140
160
180
0
20
40
60
80
100
120
140
160
180
200
220
Workpiece Radius, r_w (mm)

Figure 9.